IEEE Access
Multidisciplinary ⋮ Rapid Review ⋮ Open Access Journal

Received 14 April 2024, accepted 1 May 2024, date of publication 9 May 2024, date of current version 17 May 2024.

Digital Object Identifier 10.1109/ACCESS.2024.3398772

RESEARCH ARTICLE

Electromagnetic Transient Simulation Algorithm for Nonlinear Elements Based on Rosenbrock Numerical Integration Method

JING YE[1], JIHAO XIE[1], YONG WANG[2], LIANG ZHANG[3], BINSHAN LI[3], JINWEI LV[2], KE LI[3], SHENGPENG JIN[3], YANG XU[2], AND WEI MA[2]

[1]College of Electrical Engineering and New Energy, China Three Gorges University, Yichang 443002, China
[2]State Grid Shanghai Municipal Power Company, UHV Converter Station Branch, Shanghai 201314, China
[3]State Grid Qinghai Electric Power Company, UHV Company, Xining, Qinghai 810008, China

Corresponding author: Yong Wang (yongwang2015wy@163.com)

This work was supported by the State Grid Corporation of China (SGCC) Shanghai Electric Power Company Technology Project under Grant 52090V230002 (Quantitative Assessment Method of Transient Voltage in Station Power System Taking Into Account Commutation Failure and Hidden Disease Management of Low Voltage Control Circuit, No. 52090V230002).

ABSTRACT Traditional nonlinear elements of the electromagnetic transient simulation program (EMTP) use the numerical integration method, often employing the trapezoidal integration method as an implicit algorithm. However, when the number of nonlinear elements is high, the iterative format becomes computationally cumbersome. The semi-implicit format algorithms, based on the Rosenbrock real-time integration method, do not require iterations and can be applied directly in a recursive manner. However, as the number of nonlinear elements increases, it becomes necessary to invert the matrix that contains the Jacobian matrix, resulting in an increase of both algorithmic computation and inversion time with the dimensionality of the system. In this paper, a new numerical solution method is adopted, which combines the precise integration method. Specifically, the Calahan algorithm, with 2-stage and 3-order, is used to numerically integrate the Duhamel integration terms, and the accuracy of the Calahan algorithm is enhanced through Richardson extrapolation. The new algorithm can avoid the inverse of the matrix containing the Jacobian matrix, and the computational efficiency is equivalent to an explicit method, which greatly improves the computational efficiency of the Rosenbrock integration algorithm. The results verify the effectiveness and accuracy of the algorithm for typical power system nonlinear element electromagnetic transient simulation cases.

INDEX TERMS Electromagnetic transient, Rosenbrock algorithm, precise integration method, Calahan algorithm, Jacobian matrix.

I. INTRODUCTION

The electromagnetic transient program (EMTP) has become a fundamental tool in the planning and operation of modern power systems, and the hinge of electromagnetic transient (EMT) simulation and analysis is the numerical integration algorithm [1], [2], whereas electromagnetic transient simulation of nonlinear components is a particular challenge because it requires accurate representations and effective solutions [3]. Power systems contain a large number of nonlinear components, such as transformers, reactors, surge arresters, gas discharge tubes, varistors, etc., which are nonlinear or time-varying components. For these components, many transient problems are studied using ordinary differential equations to describe their mathematical models. Accurate simulation algorithms are necessary for power system simulation [4]. For the nonlinear ordinary differential equations in the numerical solution, the rigidity problem is more common, which, in turn, puts forward higher requirements on the stability domain of numerical integration methods [5]. Numerical integration methods commonly used in electromagnetic transient simulation of power

The associate editor coordinating the review of this manuscript and approving it for publication was Ahmed A. Zaki Diab.

systems include Euler's method, implicit trapezoidal integration method, Gear's method, Runge-Kutta (RK) method, and so on. Currently, the numerical method used in the electromagnetic transient simulation procedure for power systems is mainly the implicit trapezoidal integration method [6], [7]. However, this method has some limitations in large power network systems containing a large number of nonlinear components, especially when the nonlinear components are triangularly connected circuits, which are unable to run the program for computation [8]. In terms of numerical stability, the implicit trapezoidal integration method is A-stable but not L-stable and does not have numerical damping properties. Therefore, numerical oscillations will occur when the state variables in the network change abruptly [9].Moreover, the nonlinear implicit equations generated by nonlinear components must be solved using various types of Newton iterative methods, which makes the implicit method much more computationally intensive and difficult to compute than the explicit method.

Overall, there are still several unresolved issues of EMT simulation for nonlinear elements: 1) linearization methods for mathematical models of nonlinear components in power systems; 2) high-precision and strong-stability numerical methods for solving state space models of power systems containing nonlinear components. To solve the above problems, literature [8] proposed a Newton-Raphson method nonlinear element model, which can form the nonlinear element model and linear element model directly into the conductivity matrix, applicable to any wiring and any number of nonlinear elements. However, it needs to be re-triangulated when the parameters of the nonlinear elements are changed, which increases the amount of computation. The implicit trapezoidal integration method used in the conventional EMTP is computationally intensive and may be subject to numerical oscillations. Three new L-stable real-time (LSRT) compatible algorithms, derived from the Rosenbrock integration algorithm, have been proposed in the literature [10]. These are based on the implicit RK algorithm and use embedded Newton-Raphson iterations to make the algorithm explicit [11]. In the literature [12], a two-stage, three-order Rosenbrock-Calahan algorithm is proposed, which requires only one Jacobian matrix to be computed for each step of forward integration in the solution, improving the computational speed. The above LSRT [11] and Calahan algorithm [11] based on the Rosenbrock integration algorithm are often referred to as semi-implicit (or semi-explicit) RK algorithms. No iteration is required to solve systems of nonlinear equations, they can be directly recursive and have absolute stability. However, this type of semi-implicit format algorithm, to avoid the numerical oscillation problem associated with the additional nonlinear function in the solution formula, must calculate the analytical partial derivatives of the right function [13], that is, the Jacobian matrix, the solution is more complicated, and the solution must solve the inverse matrix, the increase in the order of the equation will lead to a significant increase in calculation time for matrix inversion. The precise integration method (PIM) [15], [16], [17] proposed by Wanxie Zhong is introduced in the literature [14], which provides a one-step explicit high-precision numerical algorithm for the time-domain analysis of nonlinear dynamical equations [16], and opens up a whole new way of calculating systems of nonlinear differential equations, which can be applied to solving systems of nonlinear differential equations in power systems.

In addition, to address the numerical oscillation problem in EMT simulations [18], [19], [20], [21], [22], [23], [24], researchers have proposed a critical damping adjustment (CDA) method by combining the implicit trapezoidal formula with the backward Euler method [25]. The CDA method can automatically switch the numerical integration algorithm to the backward Euler method during network mutations, thereby avoiding numerical oscillation in simulation results. To improve EMT simulation efficiency and avoid numerical oscillations, Reference [26] applied the three-stage implicit diagonal RK method to EMT simulations, and achieved variable order and step size of the algorithm, which has high computational efficiency. For linear switching circuits, Reference [27] proposed a standardized model establishment and solution method for linear switching circuits based on state space equations. This method uses the CDA method to avoid numerical oscillations. Reference [28] used z-transform to achieve electromagnetic transient simulation of transmission lines in the frequency domain, but it cannot be used for power systems containing nonlinear lumped parameter components [29]. Reference [30] proposed time-domain EMT simulations for transmission lines with variable frequency parameters, and this method is also applicable to simulation of circuit systems with nonlinear load components. The above methods are applicable in avoiding numerical oscillation problems, but there are still some unresolved issues for EMT simulations of large-scale power systems containing nonlinear components.

In order to solve the above problems of above references, this paper proposes a numerical method combining Rosenbrock numerical integration method and PIM for electromagnetic transient simulation with nonlinear components in power systems. The main contribution of this paper is to be summarized as follows: 1) Efficient numerical calculation without iteration is achieved for the system state space model with nonlinear components in power systems; 2) Proposed a segmented interpolation function model for nonlinear components in power systems.

In detail, the algorithm for electromagnetic transient simulation of nonlinear elements in power systems is proposed based on the Rosenbrock real-time integration algorithm, which combined with the PIM, rewrites the set of nonlinear ordinary differential equations of the power system into the form of a combination of homogeneous terms plus inhomogeneous terms and transforms them into the homogeneous integral equations according to the precise exponential

TABLE 1. Symbol table.

symbol	meaning
$\boldsymbol{I}$	unit matrix
α_i , γ , b_i	algorithm coefficients
h	integration step
$\boldsymbol{J}$	Jacobian matrix
$\boldsymbol{H}$	constant coefficient matrix
$\boldsymbol{r}(\boldsymbol{y},t)$	nonlinear generalized term

matrices. The homogeneous terms are accurately calculated by the PIM and the inhomogeneous terms are calculated by the Calahan algorithm. The numerical accuracy of the Calahan algorithm is verified by Butcher's fundamental order theorem, and the Calahan algorithm is used in combination with the Richardson extrapolation method to improve the numerical accuracy. The new algorithm can avoid solving the Jacobian matrix and inverting to $[\boldsymbol{I}-\gamma_{ii}h\boldsymbol{J}]^{-1}$. The computational efficiency is equivalent to an explicit method, which greatly improves the computational efficiency of the Rosenbrock integration algorithm. Typical simulation cases verify that the convergence, accuracy, and computational efficiency of the algorithm are higher than those of the trapezoidal integration method.

To gain a better understanding, a symbol table to explain the meaning of many of the symbols that appear in the equations is given as below.

II. ROSENBROCK REAL-TIME INTEGRATION ALGORITHM

A. COMPUTATION SCHEME OF THE ROSENBROCK ALGORITHM

The Rosenbrock integration algorithm is a class of diagonal implicit RK methods [19]. It is explicitly based on implicit RK methods using embedded Newton iterations [18], [19]. These algorithms are often referred to as semi-implicit (or semi-explicit) RK algorithms [19]. Consider the initial value problem of an m-dimensional nonlinear system of ordinary differential equations:

$$\begin{cases}\dot{\boldsymbol{y}}(t)=\boldsymbol{f}(\boldsymbol{y},t)\\ \boldsymbol{y}(t=0)=\boldsymbol{y}_0\end{cases} \tag{1}$$

In equation (1), t denotes the time variable; y is the state variable to be solved; $\boldsymbol{f}(\boldsymbol{y},t)$ is a one-dimensional function on time t and state variable $\boldsymbol{y}$; $\boldsymbol{y}_0$ is the function value of the state variable at the initial instant.

Solve the initial value problem (1) when $\boldsymbol{f}(\boldsymbol{y},\ t)$ has the necessary derivatives of each order, as described below, and $\boldsymbol{y}_k$ denotes the value of the state variable function at the time t_k. To compute the state variable value $\boldsymbol{y}_{k+1}$ at the time t_{k+1}, the s-stage Rosenbrock algorithm is used, computed in the following format [19]:

$$\boldsymbol{y}_{k+1}=\boldsymbol{y}_k+\sum_{i=1}^{s}b_i\boldsymbol{k}_i$$

$$\boldsymbol{k}_i=[\boldsymbol{I}-\gamma h\boldsymbol{J}]^{-1}\cdot[h\boldsymbol{f}(\boldsymbol{y}_k+\sum_{j=1}^{i-1}\alpha_{ij}\boldsymbol{k}_j,\ t_k+\alpha_i h)+h\boldsymbol{J}\sum_{j=1}^{i-1}\gamma_{ij}\boldsymbol{k}_j] \tag{2}$$

In the above equation (2), I is the $m\times m$ dimensional unit matrix; $\alpha_i=\sum_{j=1}^{i-1}\alpha_{ij}$, γ, γ_{ij} and b_i are the algorithm coefficients; h is the integration step, which is denoted as $h=t_{k+1}-t_k$; and $\boldsymbol{J}=\partial\boldsymbol{f}/\partial\boldsymbol{y}$ is the partial derivatives of the right function $\boldsymbol{f}$, which is called the Jacobian matrix. The method also involves s unknown quantities $\boldsymbol{k}_i$, which require s inversions of the matrix $[\boldsymbol{I}-\gamma_{ii}h\boldsymbol{J}]^{-1}$.

Based on such semi-implicit Rosenbrock integration algorithms, Bursi et al [10] proposed an L-stable real-time integration algorithm with order accuracy to satisfy the need for accuracy and simplicity of computation, only the LSRT2 (L-stable real-time two-stage method) method with two-order accuracy is analyzed in the following, and Calahan et al [12] proposed a two-stage Rosenbrock integration algorithm with three-order accuracy that can satisfy the need for engineering computation.

When the LSRT2 method is applied to the problem $\dot{y}=f(y,t)$, the coefficients of the Rosenbrock integration algorithm take the values as follows [18]:

$$\alpha_2=\alpha_{21}=1/2,\ b_1=0,\ b_2=1$$
$$\alpha_{10}=0,\ \gamma=1-\sqrt{2}/2 \tag{3}$$

For the LSRT2 method can be expressed as [18]:

$$\boldsymbol{k}_1=[I-\gamma h\boldsymbol{J}]^{-1}\cdot h\boldsymbol{f}_k,\boldsymbol{y}_{k+1/2}=\boldsymbol{y}_k+\frac{1}{2}\boldsymbol{k}_1 \tag{4}$$
$$\boldsymbol{k}_2=[I-\gamma h\boldsymbol{J}]^{-1}\cdot h(\boldsymbol{f}_{k+1/2}-\boldsymbol{J}\gamma\boldsymbol{k}_1)$$
$$y_{k+1}=y_k+k_2 \tag{5}$$

When Calahan algorithm is applied to the problem $\dot{y}=f(y,t)$, the coefficients of the Rosenbrock integration algorithm take the values as follows [18]:

$$\alpha_{10}=0,\quad \alpha_{21}=-2\sqrt{1/3}$$
$$b_1=0.75,\quad b_2=0.25\gamma\quad =\frac{1}{2}(1+\sqrt{1/3}),\quad \gamma_{21}=0 \tag{6}$$

Calahan algorithm can be expressed as [18]:

$$\boldsymbol{k}_1=[I-\gamma h\boldsymbol{J}]^{-1}\cdot h[\boldsymbol{f}_{(y_k,t_k)}+\gamma h(\frac{\partial\boldsymbol{f}}{\partial t})_{t_k}]$$
$$\boldsymbol{k}_2=[I-\gamma h\boldsymbol{J}]^{-1}\cdot h(\boldsymbol{f}_{(y_k+\alpha_{21}k_1,t_k+\alpha_{21}h)}+\gamma h(\frac{\partial\boldsymbol{f}}{\partial t})_{t_k+\alpha_{21}h}) \tag{7}$$

$$\boldsymbol{y}_{k+1}=\boldsymbol{y}_k+0.75\boldsymbol{k}_1+0.25\boldsymbol{k}_2 \tag{8}$$

In solving nonlinear systems of state equations, the semi-implicit LSRT2 method and the Calahan algorithm are both characterized by explicit recursion form, and the Calahan algorithm is a three-order numerical accuracy algorithm,

which is one order higher than the LSRT2 method. The Calahan algorithm is chosen to solve the specific problem studied in this paper, but the difficulties in solving the engineering problem are as follows: in engineering computation, when there are more nonlinear components, the analytic partial derivatives of the right function should be used in the solution formula to find its Jacobian matrix and the numerical partial derivatives cannot be used to ensure the absolute stability of the solution, and the solution of Jacobian matrices is more complicated. The Jacobian matrix is more complicated to solve; the inverse of the Jacobian matrix and the $[\boldsymbol{I}-\gamma_{ii}h\boldsymbol{J}]^{-1}$ matrix is required for the solution, and the time to solve the inverse of the Jacobian matrix increases quadratically as the order of the equation increases.

To avoid solving the Jacobian matrix and inverting the $[\boldsymbol{I}-\gamma_{ii}h\boldsymbol{J}]^{-1}$ matrix, the Calahan algorithm is combined with the PIM to solve the multidimensional nonlinear state equation. For the m-dimensional nonlinear system of ordinary differential equations, equation (1) can be rewritten as a combination of homogeneous terms plus inhomogeneous terms:

$$\begin{aligned}&\dot{\boldsymbol{y}}=\boldsymbol{H}y+\boldsymbol{r}(\boldsymbol{y},t)\quad\text{(a)}\\&\boldsymbol{y}_{k+1}=e^{h\boldsymbol{H}}\boldsymbol{y}_k+\int_{t_k}^{t_{k+1}}e^{\boldsymbol{H}(t_{k+1}-\xi)}\boldsymbol{r}(\boldsymbol{y}_{(\xi)},\xi)d\xi\quad\text{(b)}\end{aligned}\tag{9}$$

In equation (9), $\boldsymbol{H}$ is the m-dimensional constant coefficient matrix; $\boldsymbol{r}(\boldsymbol{y},t)$ is the nonlinear generalized term.

The solution to the system of m-dimensional nonlinear ordinary differential equation can be expressed in the uniform integral equation as equation in an arbitrary integration interval $[t_k,t_{k+1}]$ using the exponential matrix [16].

The initial homogeneous term on the right-hand side of equation (9b) can be precisely computed using the 2^N class precise integration algorithm [15]. The second Duhamel inhomogeneous integration term can be obtained by Calahan algorithm as follows:

$$\boldsymbol{F}(t)=\int_{t_0}^{t}e^{\boldsymbol{H}(t-\xi)}\boldsymbol{r}(\boldsymbol{y}_{(\xi)},\xi)d\xi\tag{10}$$

$$\begin{cases}\dot{\boldsymbol{F}}(t)=e^{\boldsymbol{H}(t-t_0)}\boldsymbol{r}(\boldsymbol{y},t)\\ \boldsymbol{F}(t_0)=\boldsymbol{r}(\boldsymbol{y}_0,t_0)\end{cases}\tag{11}$$

In solving the Jacobian matrix for solving initial value problem (11) by Calahan algorithm, since the right-hand function in equation (11) does not explicitly contain the state variable $\boldsymbol{F}$, thus the Jacobian matrix of equation (11) is $\boldsymbol{J}=\boldsymbol{0}$. This method transforms the differential equation into an integral equation and the numerical solution of equation (11), i.e. the integral of the inhomogeneous terms in equation (9), is calculated according to equation (6) and (7).

The Jacobian matrix and the inversion of the $[\boldsymbol{I}-\gamma_{ii}h\boldsymbol{J}]^{-1}$ matrix can be avoided when solving with the Calahan algorithm, and the explicit fourth-order RK algorithm can be used to predict the value of $\boldsymbol{y}$ in $\boldsymbol{r}(\boldsymbol{y},t)$. The overall computational format of the algorithm is equivalent to an explicit method, which greatly improves the computational efficiency of the Rosenbrock integration algorithm.

B. NUMERICAL ACCURACY AND STABILITY OF THE ROSENBROCK ALGORITHM

To study the numerical accuracy of the s-stage Rosenbrock algorithm, the simplified order conditions derived from Butcher's theory of rooted tree structures [19] are used:

$$\begin{cases}B(p):\sum_{i=1}^{s}b_ic_i^{k-1}=\frac{1}{k},k\in(1,p)\\ C(\eta):\sum_{j=1}^{s}a_{ij}c_j^{k-1}=\frac{c_i^k}{k},i\in(1,s),k\in(1,\eta)\\ D(\zeta):\sum_{i=1}^{s}b_ic_i^{k-1}a_{ij}=\frac{b_j}{k}(1-c_j^k),j\in(1,s),\\ k\in(1,\zeta)\end{cases}\tag{12}$$

According to equation (2), for the s-stage Rosenbrock algorithm, denote $c_1=\alpha_{10},c_i=\sum_{j=1}^{i-1}\alpha_{ij},i\in(2,s),a_{ij}=\alpha_{ij}$; then we have $\boldsymbol{A}=(a_{ij})$, $\boldsymbol{b}=(b_i)^T$ and $\boldsymbol{c}=(c_i)$. Combined with Butcher's simplified order condition, there is the following Butcher's fundamental order theorem, i.e. [19]:

Theorem: If the coefficients of an s-stage RK method satisfy the simplified order condition (12) with $p\le\eta+\zeta+1$ and $p\le2\eta+2$, then the s-stage RK method is p-order.

Based on Butcher's fundamental order theorem, it can be verified that the accuracy of the LSRT2 method and Calahan algorithm are of 2nd and 3rd order respectively.

The second and third order accuracy currently used in the Rosenbrock algorithm is not high enough. To improve the numerical integration accuracy of the Rosenbrock algorithm, the Calahan algorithm is used in conjunction with Richardson extrapolation [19]. For a p-order method, the numerical solution at the point t_{k+1} with time step-size h is denoted as $y_{k+1}(h)$, the numerical solution at the same point t_{k+1} with time step-size $h/2$ is denoted as $y_{k+1}(h/2)$, and the exact solution of the differential equation at the point t_{k+1} is denoted as y_{k+1}:

$$\begin{cases}y_{k+1}(h)-y_{k+1}=h^p\varepsilon(t_{k+1})+O(h^{p+1})\\ y_{k+1}(h/2)-y_{k+1}=(h/2)^p\varepsilon(t_{k+1})+O(h^{p+1})\end{cases}\tag{13}$$

where, $\varepsilon(t_{k+1})$ in the above equation (13) is the main error function. The above equation can be obtained by simplification of equation (13):

$$y_{k+1}=\frac{2^py_{k+1}(h/2)-y_{k+1}(h)}{2^p-1}+O(h^{p+1})\tag{14}$$

$$\varepsilon(t_{k+1})=\frac{2^p[y_{k+1}(h)-y_{k+1}(h/2)]}{2^p-1}\tag{15}$$

where, y_{k+1} of the above equation (14) as a new numerical solution has an error of $O(h^{p+1})$ compared to the exact solution of the differential equation, which eliminates the main error term and improves the local calculation accuracy of the numerical algorithm. When using extrapolation, its time step-size h can be increased to $10h$ to achieve the same accuracy as when calculating with a step size of h. It is reasonable

to improve the time accuracy by Richardson extrapolation. Meanwhile, during the calculation, if $\varepsilon(t_{k+1})$ is within the allowable error range, the calculation time can be saved by increasing the time step-size.

To analyze the stability of the Calahan algorithm, consider applying the Calahan algorithm to the following scalar test equation [18]:

$$\begin{cases} \dot{y} = \lambda y \\ y(t_0) = y_0 \end{cases} \tag{16}$$

In the above equation (16), $\mathrm{Re}(\lambda) < 0$. Assuming $J = \partial f/\partial y = \lambda$ and letting $z = h\lambda$, $h > 0$, the difference equation is obtained:

$$y_{k+1} = R(z) \cdot y_k \tag{17}$$

where, $R(z)$ in equation (17) above is a rational fractional function of z.

Definition [19]: A numerical integration formula is defined as infinitely stable if the following condition is satisfied: there exists a real number $\sigma < 0$ such that the sequence $\{y_k\}$ obtained by applying the formula to equation (15) at a defined step-size $h > 0$ satisfies:

$$\sup_{\mathrm{Re}(z)<\sigma} \left| \frac{y_{k+1}}{y_k} \right| = \vartheta < 1 \tag{18}$$

In the above equation (18), $\sup |y_{k+1}/y_k|$ denotes the upper bound ϑ of $|y_{k+1}/y_k|$.

According to the above definition of infinite stability, the Calahan algorithm is infinitely stable if it exists $|R(z)| < 1$ when $\mathrm{Re}(z) < 0$ [18]. To prove the above conclusion, it is only necessary to show that if $\mathrm{Re}(z) \to -\infty$, $|R(z)| < 1$.

Equation (19) is obtained by combining the calculations in equation (7):

$$\begin{aligned} y_{k+1} = y_k &+ 0.75[I - \gamma h\lambda]^{-1} \cdot h\lambda y_k + 0.25[I - \gamma h\lambda]^{-1} \\ &\cdot h[\lambda(y_k + 0.75\alpha_{21}[I - \gamma h\lambda]^{-1} \cdot h\lambda y_k)] \end{aligned} \tag{19}$$

Equation (20) can be obtained by associating it with equation (18):

$$R(z) = \frac{1 - 0.578z - 0.456z^2}{1 - 1.578z + 0.622z^2} \tag{20}$$

For $\mathrm{Re}(z) \to -\infty$, there is $|R(z)| \approx 0.733 < 1$, so the Calahan algorithm is infinitely stable.

III. ELECTROMAGNETIC TRANSIENTS SIMULATION ALGORITHM FOR NON-LINEAR COMPONENTS

The numerical integration method in the traditional electromagnetic transient simulation program EMTP is usually the 2nd order A-stable implicit trapezoidal integration method, which may suffer from numerical oscillations when the simulation step size is insufficient. The Calahan algorithm combined with the PIM proposed in this paper rewrites the m-dimensional nonlinear ordinary differential equation system as a combination of homogeneous and inhomogeneous, solves the homogeneous terms by the PIM, solves the inhomogeneous terms by the Calahan algorithm, and improves its numerical accuracy by Richardson extrapolation. This method can be applied to the numerical calculation of electromagnetic transient simulation of the power system to avoid solving the complex Jacobian matrix and eliminate the limitations of the traditional EMTP method, which can achieve the same accuracy by increasing the step size, which not only improves the computational efficiency but also avoids the numerical oscillation due to the large step size. The specific steps of the simulation algorithm are as follows:

1) Nonlinear component modeling process. For the common nonlinear resistance or nonlinear inductance in the power system network, its instantaneous characteristic curve is calculated according to its conventional experimental data, and then the curve is approximated numerically, and the commonly used methods are segmented linear method and function fitting method;

2) Original parameters of the power system preparation process. Set up a system of ordinary differential equations for each element of the circuit, and form the $m \times m$-dimensional coefficient matrix $\boldsymbol{H}(\boldsymbol{y}, t)$. The quantities in the coefficient matrix $\boldsymbol{H}(\boldsymbol{y}, t)$ that are related to the time t and the state variable $\boldsymbol{y}$ are grouped into $\boldsymbol{r}(\boldsymbol{y}, t)$, and the constant coefficient matrix $\boldsymbol{H}$ is constructed, which leads to the formation of a unified form of electromagnetic transient numerical calculation of the mathematical model $\dot{\boldsymbol{y}} = \boldsymbol{H}\boldsymbol{y} + \boldsymbol{r}(\boldsymbol{y}, t)$ (denoted as initial value problem ①) [20], [21];

3) Initialization process. Setting the initial simulation moment $t = 0.0s$ and the number of integration steps $k = 0$. Setting the numerical integration fixed step length h and the total time T of electromagnetic transient simulation computation. Setting the initial value of each state variable in the system, i.e. $\boldsymbol{y}(t = 0) = \boldsymbol{y}_0$;

4) Numerical integration process. the Calahan algorithm combined with the PIM is used to calculate the value $\boldsymbol{y}_{k+1}$ of the state variable at $t = t_{k+1} = t_k + h$;

5) Process of increasing simulation steps. Let $t_{k+1} = t_k + h$; $k = k + 1$;

6) Process of determining whether to stop the simulation or not. If $t < T$, go to Step 4 and continue the numerical integration at the next moment, if $t \geq T$, go to Step 7;

7) Output of numerical simulation results of electromagnetic transients.

The specific process for modeling a nonlinear component in Step 1 above is as follows: segmented linear method and function fitting method are two commonly used mathematical modeling tools. Based on the characteristic curve $u - x$ of a nonlinear resistor or inductor, a function is found to describe this curve and the fitting function can be a power function as shown in equation 21(a) below, or a hyperbolic sine function [22] as shown in equation 21(b) below:

$$\begin{aligned} u(x) &= Ax^B \text{(a)} \\ u(x) &= A\sinh(Bx) \text{(b)} \end{aligned} \tag{21}$$

Using a single function to fit the nonlinear characteristics may be too saturated compared to the original curve. For part

TABLE 2. Selected data points from the volt-ampere characteristic of the Model S10K250 Varistor.

Amps/A	Volts/V (p.u.)
0.001	1.808
0.01	1.9883
0.1	2.1056
1	2.2316
10	2.3844
20	2.4355
30	2.4708

*Reference value 250V.

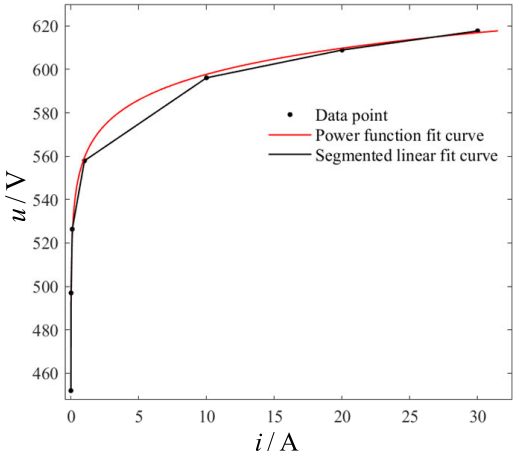

FIGURE 1. S10K250 Varistor volt-ampere characteristic curve.

of the nonlinear component characteristic curve with fewer segments, the fitting accuracy is not high, this paper adopts the combination of segmented linear method and function fitting method to improve the fitting accuracy. That is, the front of the characteristic curve segment linear and inflection section can be used function fitting method, while the saturated section of the characteristic curve behind the linear fitting, so that the fitting accuracy is higher. The volt-ampere characteristic curve of the S10K250 type varistor shown in Table 2 is used as an example for numerical simulation, and its segmented linear fit curve and function fit curve are shown in Figure 1.

In the above Step 4, the Calahan algorithm combined with the PIM to solve the initial value problem ① is as follows: for the mathematical model formed in Step 2, the first homogeneous term can be solved by PIM; and the second Duhamel inhomogeneous integrator is calculated by the Calahan algorithm, which is used in combination with Richardson extrapolation method to improve the accuracy of numerical integration.

IV. CASE STUDY

A. ANALYSIS OF AC CONTROL LOOP WITH VARISTOR

This case is the electromagnetic transient simulation analysis of the AC control loop of the converter transformer cooler in a converter station. As shown in Figure 2, the varistor inside the TC180 key module of the AC control loop of the converter

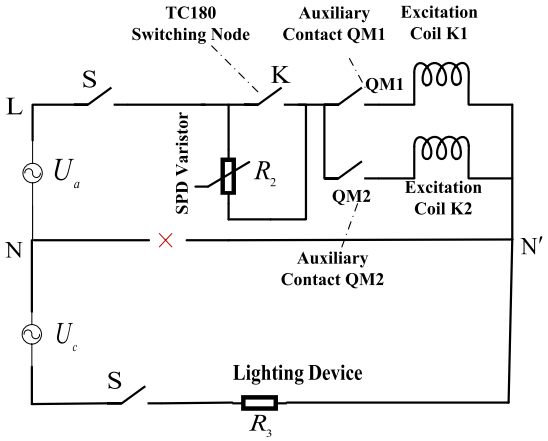

FIGURE 2. Starting and stopping control circuit of converter transformer cooler.

transformer cooler is often burned after overvoltage, which seriously affects the normal operation of the cooler. After the failure phenomenon and equipment data collection in the early stage, there are 2 types of reasons for analyzing the frequent occurrence of varistor burnout in this circuit:

(1) Type 1: There is an isolation point in the load neutral. As shown in Figure 3, there is an isolation point between the neutral. Since the load neutral cannot clamp the zero potential, the AC system failure occurs in winter, HVDC system transmission power is relatively small, the converter transformer coolers only need to start one group, the other two groups of coolers in the shutdown state (i.e. node K in the disconnected state). A group of coolers corresponding to the varistor R_2 (provided that K is not closed) and other lighting load resistor R_3 series voltage division U_{ab}, due to the a-phase load of the five excitation coils are connected in parallel, resulting in the total resistance being very small, so there is almost no share of the voltage. At this point, the varistor R_2 is subjected to a very high transient overvoltage and then operates, causing a high current to flow and burn out. This happens when there is a single-phase load other than the a-phase load;

(2) Type 2: Fault current flowing into the load neutral. As shown in Figure 3, it is assumed that the three-phase load is asymmetrical and there is no separation point between the neutral lines. Since the low-voltage side neutral point of the dry-type transformer Dyn11 of the former power supply is directly earthed, if there is a short-circuit fault to earth in the other single-phase loads, the fault current will flow into the neutral through the earth, and in the extreme case, the other loads are disconnected, which will cause the fault current to flow through the varistor R_{SPD}, but at this time the resistance value of the varistor is relatively large, resulting in burn-out due to the sharp rise in heat.

To verify the nature of the faults leading to varistor burnout, an equivalent circuit diagram of the converter transformer cooler start-stop control loop was constructed as shown in Figure 3 based on Type 1, and its Thevenin equivalent circuit

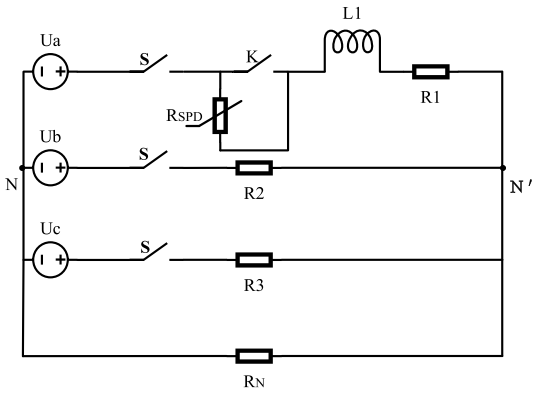

FIGURE 3. Equivalent circuit diagram of the start stop control circuit of the converter transformer cooler.

diagram was obtained under the condition of neutral linear disconnection as shown in Figure 4.

As shown in Figure 3, $R_1 = 42.8\Omega$, $R_2 = 150\Omega$, $R_3 = 275\Omega$, $R_N = 1\Omega$, $L_1 = 42.8mH$; R_{SPD} denotes a varistor.

As shown in Figure 4, R_{eq} and u_{oc} are shown below when the neutral is disconnected:

$$\begin{cases} R_{eq} = 1 \Big/ \left(\dfrac{1}{R_2} + \dfrac{1}{R_3}\right) \\ u_{oc} = u_a - \left(\dfrac{u_b}{R_2} + \dfrac{u_c}{R_3}\right) R_{eq} \end{cases} \tag{22}$$

where u_a, u_b and u_c are the voltages of each phase of the three-phase supply, R_{eq} is the Thevenin equivalent resistance, u_{oc} is the Thevenin equivalent voltage, and R_N is the neutral resistance.

The segmented linear fitting curve and the function fitting curve are used to mathematically model the varistor R_{SPD}, and the electromagnetic transient simulation algorithm with nonlinear components proposed in this paper is used to perform the electromagnetic transient simulation analysis of the control loop. The simulation conditions are as follows: the varistor is fitted with a segmented linear fitting curve, the station bus voltage is 520V, the calculation time-step size $h = 1.0 \times 10^{-5}s$ of the Calahan algorithm and the 2^N of N type fine integration algorithm is taken as 15; the calculation time-step of the trapezoidal method is $h = 1.0 \times 10^{-6}s$, and the simulation results are shown in Figure 5(a); and the results of the calculation time-step of the two methods when both are taken as $h = 1.0 \times 10^{-5}s$ are shown in Figure 5(b). From the simulation results in Figure 5, it can be seen that the peak current flow through the varistor is approximately 960mA, indicating that the varistor has been operated. Both algorithms produce numerical oscillations in the simulation, and the Calahan algorithm produces numerical oscillations to a lesser extent than the trapezoidal method at the same computational time-step; the advantage of the Calahan algorithm lies in the fact that it can be used in electromagnetic transient simulation with a larger computational time-step, and the computational efficiency is better than that of the trapezoidal method. The rest of the simulation conditions remain unchanged, and the voltage-ampere characteristic curve of the

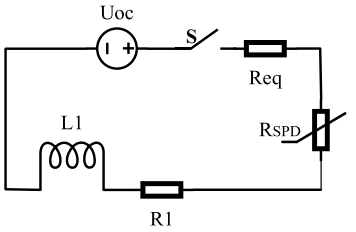

FIGURE 4. Thevenin equivalent circuit diagram during cooler shutdown.

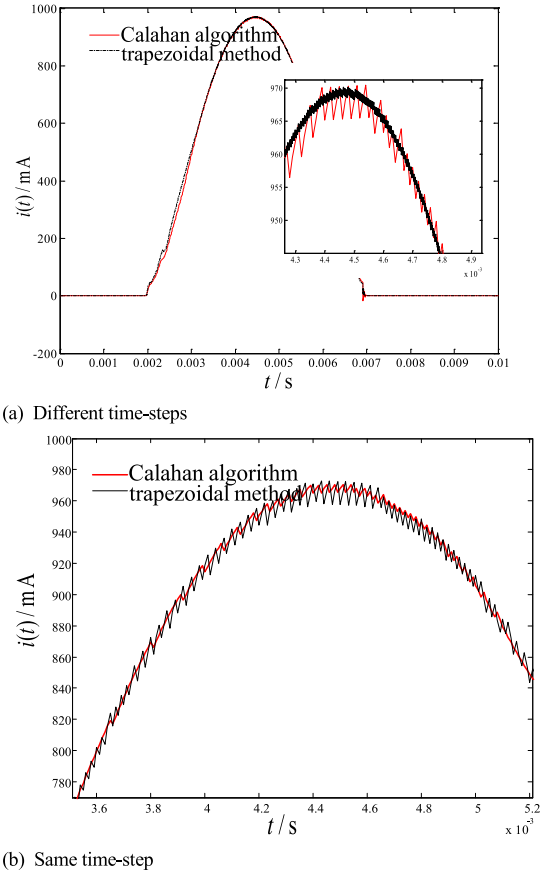

(a) Different time-steps

(b) Same time-step

FIGURE 5. Simulation results of two algorithms (piecewise linear model).

varistor is fitted by the following power function model:

$$u_{spd} = Ki_{spd}^m \tag{23}$$

where, $K = 558.6$, $m = 0.02863$; i_{spd} is the varistor current (A) and u_{spd} is the varistor voltage (V).

The piezo resistor uses the power function model of equation (23) and the calculation results when both calculation time-steps are taken as $h = 1.0 \times 10^{-6}s$ are shown in Figure 6. At this time, the peak current flow through the varistor is about 550mA, which shows that the varistor has been acted upon. The simulation results of the two do not produce numerical oscillations and the trajectories of the current curves calculated by the two are basically coincident. This suggests that the varistor characteristic curve using continuous function model fitting can avoid the problem of numerical oscillation.

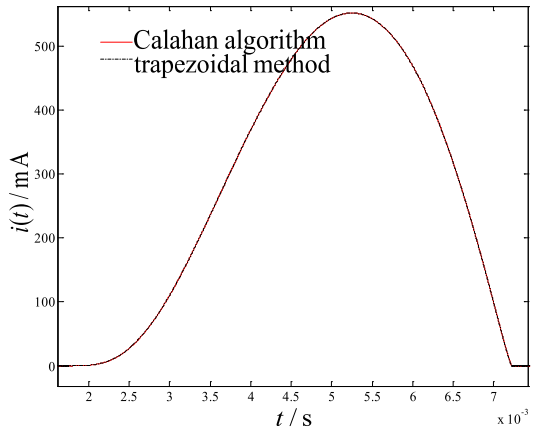

FIGURE 6. Simulation results of two algorithms (power function model).

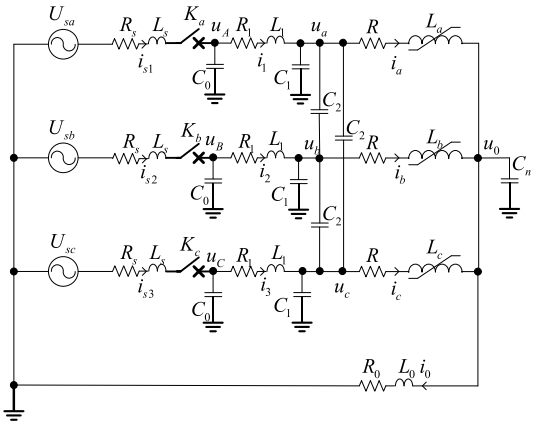

FIGURE 7. Circuit diagram of three equal values for no-load closing of 110kV transformer busbar.

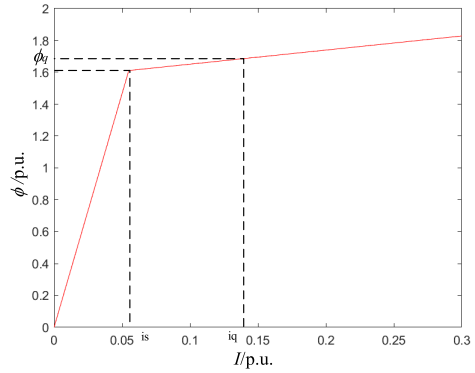

FIGURE 8. Piecewise linear model of excitation curve.

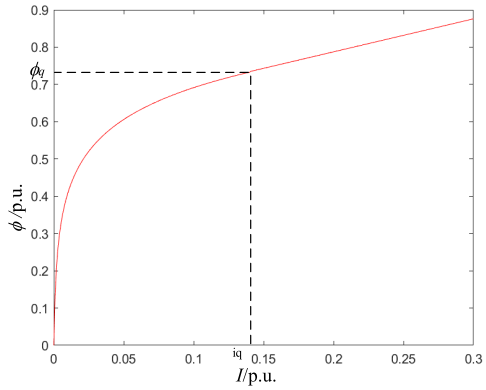

FIGURE 9. Function fitting model of excitation curve.

B. POWER TRANSFORMER INRUSH ANALYSIS

This case is the electromagnetic transient simulation analysis of the 110kV transformer closing operation of a substation. According to the actual parameters of 110kV transformer electrical equipment calculated transmission line equivalent capacitance, reactance, resistance, line capacitance between phases; transformer winding input capacitance, neutral equivalent capacitance, nonlinear winding inductance, and other parameters, the specific value of the relevant parameters see the literature [21]. According to the specific parameters calculated above to establish the actual 110kV transformer bus no-load closing three-phase equivalent circuit calculation model shown in Figure 7.

When calculating the inductance of a nonlinear transformer winding, the segmented linear method or the function fitting method is generally used. The $\phi - i$ magnetization curve of the transformer winding is divided into two sections of linear inductance slope and saturated inductance slope by the segmented linear method, as shown in Figure 8, and the $\phi - i$ magnetization curve is described by the power function or hyperbolic sinusoidal function by the function fitting method. The two-segment linear method is not accurate, and the function fitting curve is too saturated compared with the original curve, this case uses the segment fitting method to improve the accuracy [22], [23], [24], the $\phi - i$ magnetization curve is divided into three segments, the front of the linear segment and the inflection segment using hyperbolic sinusoidal function $u(x) = Ash(By)$ fitting, the back of the saturated segment using a straight line to fit, the transformer inductance of the nonlinear windings fitted curve as shown in Figure 9.

The excitation winding characteristics of the power transformer using a segmented linear model, as shown in Figure 8; the excitation winding characteristics using a hyperbolic sinusoidal function and a linear function combination model (three-segment model), as shown in Figure 9. The simulation conditions are set as follows: as shown in Figure 7, the bus power a-phase circuit breaker K_a is closed first at $t = 0.02s$, and then the B-C two-phase circuit breaker is closed at the same time after half a weekly wave, at this time, the calculation time-step of the Calahan algorithm is 10 microseconds, and the simulation results are shown in Figure 10. Similarly, the excitation winding characteristics using a three-segment model, and other simulation conditions remain unchanged, the simulation results are shown in Figure 11, at this time, the three-phase high-voltage side of the voltage waveform produces serious numerical oscillations. And the second harmonic accounts for the main proportion of voltage waveform in Figure 11(b). After low-pass filtering the waveform, obvious overvoltage phenomena can be seen in Figure 11(b). Comparing the simulation results in Figures 10 and 11,

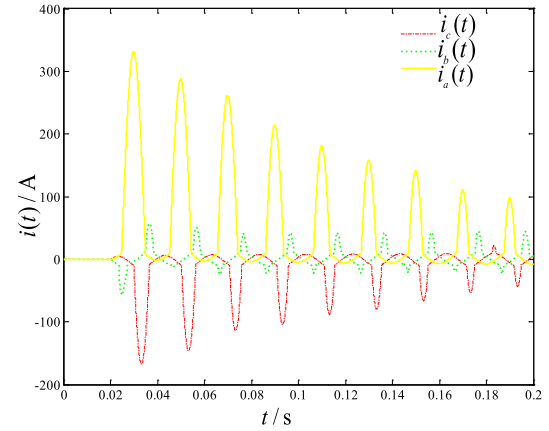

(a) Three-phase excitation inrush waveforms

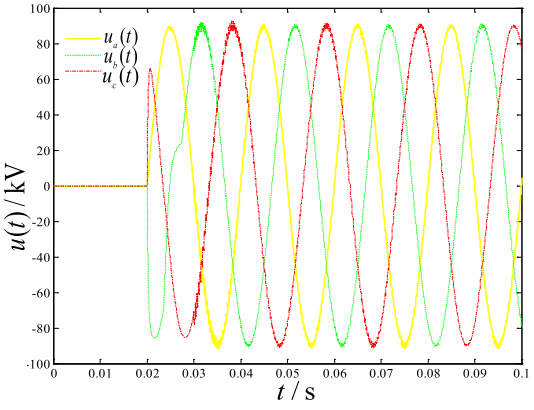

(b) Three-phase high-voltage side voltage waveforms

FIGURE 10. Voltage and current waveforms of transformer no-load closing (piecewise linear model).

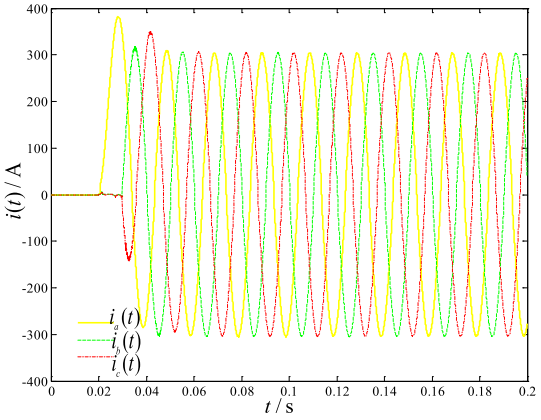

(a) Three-phase excitation inrush waveforms

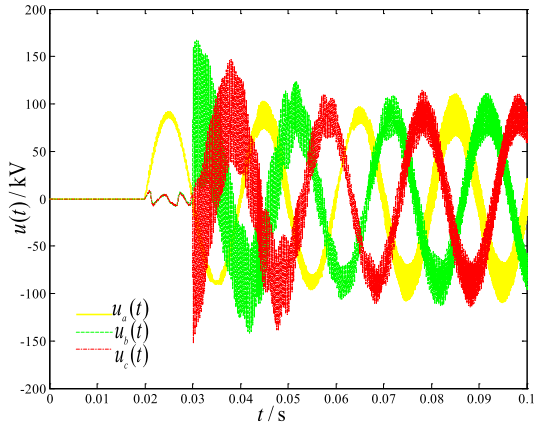

(b) Three-phase high-voltage side voltage waveforms

FIGURE 11. Voltage and current waveforms of transformer no-load closing (three-segment model).

the Calahan algorithm is better than the segmented linear model, but if the numerical algorithm with L-stability is used, the numerical oscillations of the voltage waveform can be avoided, and the simulation results are more accurate when the excitation winding is used in the three-segment model.

C. SIMULATIONS FOR OVER-VOLTAGES OF TRANSMISSION LINE

This case is the electromagnetic transient simulation of a transmission line without load being switched-in suddenly. Figure 12 shows the breaker of a single-phase high-voltage transmission line is switched-in at t=0s with the terminal of the line without load. In Figure 12, $R_s = 5\Omega$, $L_s = 0H$. The voltage level of the transmission line system is 220kV, therefore the reference voltage is 179.6kV. The distribution parameters of the long transmission line can be found in reference [7].

In this case, we divide the whole transmission line into 30 sections. For each unit, a lumped $\prod$ type equivalent circuit is used for modeling. Besides, the initial phase angle of voltage source signal is 90°. For comparison, we would give out the results of both Calahan algorithm, implicit trapezoidal method and CDA method. The integration step of implicit trapezoidal method and CDA method is $h = 10\mu s$,while the integration step of Calahan algorithm is $50\mu s$.For CDA

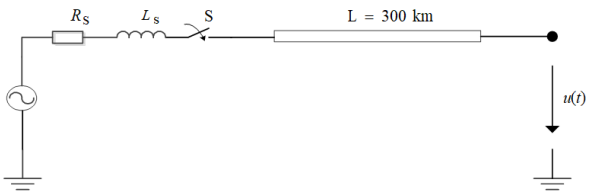

FIGURE 12. Schematic diagram of a transmission line without load being switched-in suddenly.

method, the backward Euler method is used for numerical integration from 0 to 0.002 seconds, and the implicit trapezoidal method is used for numerical integration after 0.002 seconds. The problem with the CDA method lies in detecting the moment of sudden changes in system state variables, which is often difficult for certain scenarios.

By combining the technique of increasing the dimensionality of system state variables, the non-homogeneous linear differential equations of the transmission line system can be transformed into homogeneous forms, which greatly facilitates the calculation process of the Calahan algorithm.

Comparing the simulation results in Figure 13, based on the power supply voltage, the maximum transient overvoltage value of the terminal voltage is 2.0523 p.u., and the stable overvoltage value is 1.0834 p.u., and simulation results of the Calahan algorithm is better than implicit trapezoidal method

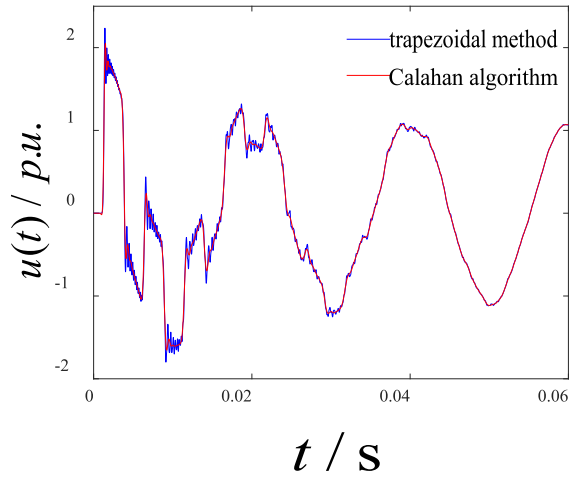

(a) Terminal voltage waveforms calculated by implicit trapezoidal method and Calahan algorithm

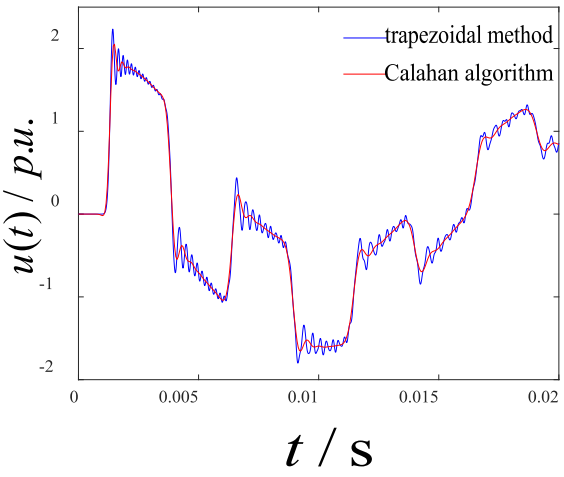

(b) Partial enlarged version of Figure 13-a

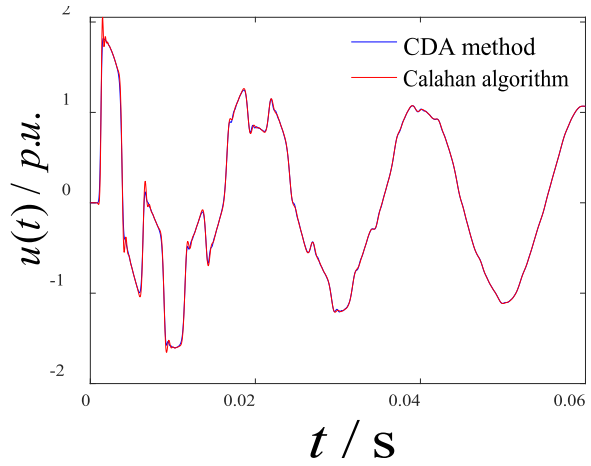

(c) Terminal voltage waveforms calculated by CDA method and Calahan algorithm

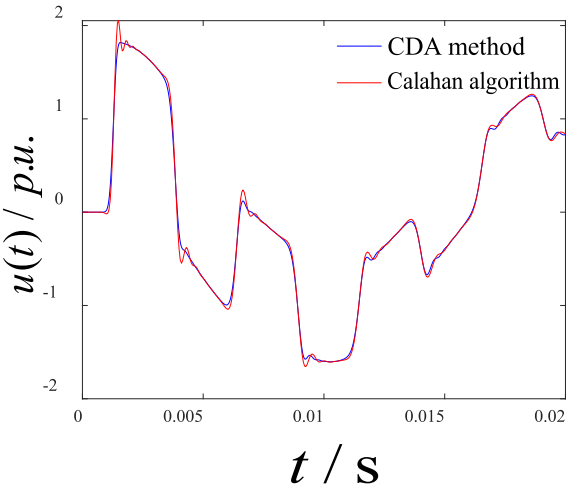

(d) Partial enlarged version of Figure 13-c

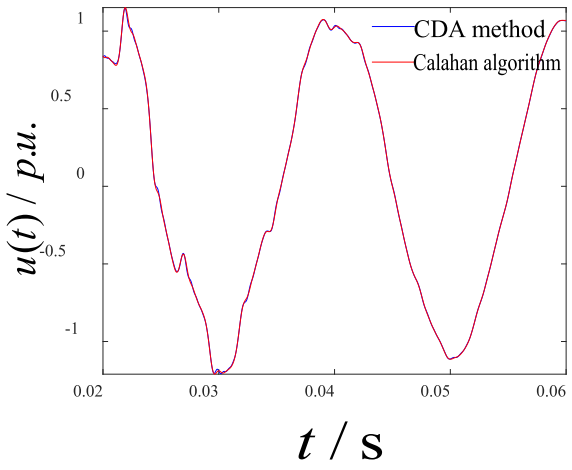

(e) Partial enlarged version of Figure 13-c

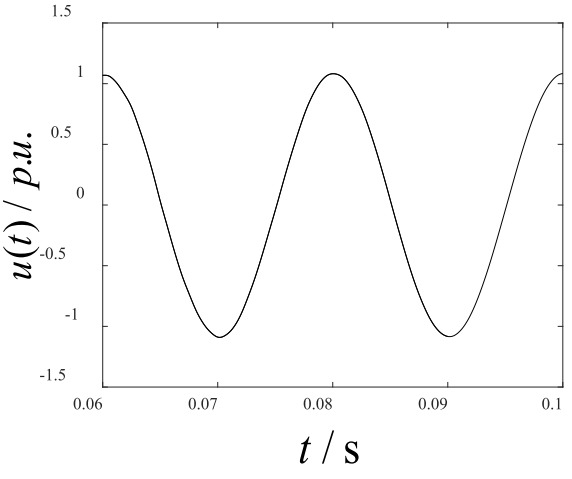

(f) Terminal voltage waveform calculated by Calahan algorithm

FIGURE 13. Terminal voltage waveforms of the transmission line.

and CDA method. As shown in Figure 13(a) and 13(b), due to the use of larger time-step, the numerical oscillation of terminal voltage waveform calculated by Calahan algorithm can be avoided. As shown in Figure 13(c) and 13(d), due to the use of CDA method and Calahan algorithm, the numerical oscillation of terminal voltage waveform calculated by these methods can be avoided. Meanwhile, as shown in Figure 13(e), due to the higher calculation accuracy of Calahan algorithm, the accuracy of terminal voltage calculation is guaranteed compared with CDA method.

V. CONCLUSION

Aiming at the problems of the numerical integration algorithm used in the traditional electromagnetic transient simulation of nonlinear elements, a new algorithm based on the Rosenbrock real-time integration algorithm for solving this problem is proposed in this paper.

The proposed new numerical algorithm specifically adopts the Calahan algorithm combined with the PIM for numerical integration. First, the system of nonlinear ordinary differential equations of the power system is transformed into its uniform integral equations, which are accurately computed by the PIM for the homogeneous terms, and the Duhamel inhomogeneous integration terms are computed by the Calahan algorithm. The numerical accuracy of the Calahan algorithm is verified by Butcher's Fundamental Order Theorem and shown to be infinitely stable, and the Calahan algorithm is combined with the Richardson extrapolation method to improve the accuracy of its numerical integration.

Numerical results show that the electromagnetic transient simulation algorithm proposed in the paper produces numerical oscillations to a lesser extent than the traditional trapezoidal integration method in the same computational time-step. The use of a continuous function fitting model for the characteristics of nonlinear components can avoid numerical oscillations in the simulation results, and the use of a segmented function fitting model can lead to numerical oscillations in the computational results in some cases.

In brief, the new algorithm can use a larger computational time step-size for electromagnetic transient simulation, and its computational efficiency and accuracy are better than that of the trapezoidal method. The advantage of the algorithm in this paper is that it can avoid solving the Jacobian matrix and inverse matrix $[\boldsymbol{I} - \gamma_{ii} h \boldsymbol{J}]^{-1}$. The computational efficiency is equivalent to an explicit numerical method, which greatly improves the computational efficiency of the Rosenbrock integration algorithm.

REFERENCES

[1] Y. Ming, Z. Yongming, and Z. Ziqian, "Review of electromagnetic transient simulation algorithms for power system," *Elect. Meas. Instrum.*, vol. 59, no. 8, pp. 10–19, 2022.

[2] Y. Tanaka and Y. Baba, "Study of a numerical integration method using the compact scheme for electromagnetic transient simulations," *Electr. Power Syst. Res.*, vol. 223, Oct. 2023, Art. no. 109666.

[3] Z. Shen and V. Dinavahi, "Dynamic variable time-stepping schemes for real-time FPGA-based nonlinear electromagnetic transient emulation," *IEEE Trans. Ind. Electron.*, vol. 64, no. 5, pp. 4006–4016, May 2017.

[4] B. Jing, Z. Zhijian, and W. Wei, "Comparative study on different algorithms of starting process of high-voltage induction motor in new power system," *Elect. Meas. Instrum.*, vol. 60, no. 7, pp. 70–76, 2023.

[5] C. Lirong and L. Degui, "Parallel Rosenbrock method for solving rigid ordinary differential equations," *Comput. Math.*, vol. 20, no. 3, pp. 251–260, 1998.

[6] J. Tant and J. Driesen, "On the numerical accuracy of electromagnetic transient simulation with power electronics," *IEEE Trans. Power Del.*, vol. 33, no. 5, pp. 2492–2501, Oct. 2018.

[7] F. Z. Wang and M. Yang, "Fast electromagnetic transient simulation for over-voltages of transmission line by high order Radau method and V-transformation," *IET Gener., Transmiss. Distrib.*, vol. 10, no. 14, pp. 3639–3645, 2016.

[8] W. Kui and S. Ying, "Modeling and simulation of nonlinear component algorithm," *Power Syst. Clean Energy*, vol. 26, no. 12, pp. 34–37, 2010.

[9] Z. Jing, Y. Jing, and Y. Ming, "Fast simulation study of nonlinear electromagnetic transients based on multi-level higher-order differential product method," *Elect. Meas. Instrum.*, vol. 60, no. 2, pp. 60–68, 2023.

[10] O. S. Bursi, A. Gonzalez-Buelga, L. Vulcan, S. A. Neild, and D. J. Wagg, "Novel coupling Rosenbrock-based algorithms for real-time dynamic substructure testing," *Earthq. Eng. Struct. Dyn.*, vol. 37, no. 3, pp. 339–360, Mar. 2008.

[11] J. Chuanguo, L. Yingmin, and Y. Pu, "Accuracy and stability analysis of Rosenbrock real-time integration method and its application in structural dynamics," *Chin. J. Appl. Mech.*, vol. 29, no. 5, pp. 566–572, 2012.

[12] D. A. Calahan, "A stable, accurate method of numerical integration for nonlinear systems," *Proc. IEEE*, vol. 56, no. 4, p. 744, Mar. 1968.

[13] C. Zhe, W. Yuanfang, and L. Guojun, "Calahan numerical calculation and dynamic simulation of inrush current of transformer excitation," *High Voltage Technol.*, vol. 30, no. 10, pp. 12–14, 2004.

[14] L. Hexiang, Y. Hongjie, and Q. Chunhang, "An integral equation of nonlinear dynamics and its solution method," *Chin. J. Solid Mech.*, vol. 22, no. 3, pp. 303–308, 2001.

[15] Z. Wanxie, "On precise time-integration method for structural dynamics," *J. Dalian Univ. Technol.*, vol. 34, no. 2, pp. 131–136, 1994.

[16] L. Dongbing, W. Yong, and Li Bowen, "An improved precise integration single-step method for nonlinear dynamic equations," *J. Vib. Shock*, vol. 41, no. 5, pp. 182–188, 2022.

[17] C. Zhiqin, "Precise time-integration methods and their partial evolution," Ph.D. dissertation, Dept. Eng. Mech., Dalian Univ. Technol., Dalian, China, 1998.

[18] G. G. Dahlquist, "A special stability problem for linear multistep methods," *BIT Numer. Math.*, vol. 3, no. 1, pp. 27–43, Mar. 1963.

[19] L. Degui, *Digital Simulation Methods of Rigid Large Systems*. Henan, China: Henan Science and Technology Press, 1996.

[20] Z. Jinli, L. Juntao, and Li Peng, "GPU based parallel algorithm oriented to exponential integration method for electromagnetic transient simulation," *Automat. Electr. Power Syst.*, vol. 42, no. 6, pp. 113–119, 2018.

[21] C. Wang, X. Fu, P. Li, J. Wu, and L. Wang, "Multiscale simulation of power system transients based on the matrix exponential function," *IEEE Trans. Power Syst.*, vol. 32, no. 3, pp. 1913–1926, May 2017.

[22] C. Zhe, "Research on transient state of power transformer and current limiting fuse based on Calahan numerical algorithm," Ph.D. dissertation Huazhong Univ. Sci. Technol., Wuhan, China 2006.

[23] W. Nzale, J. Mahseredjian, X. Fu, I. Kocar, and C. Dufour, "Improving numerical accuracy in time-domain simulation for power electronics circuits," *IEEE Open Access J. Power Energy*, vol. 8, pp. 157–165, 2021.

[24] S. Subedi, M. Rauniyar, S. Ishaq, T. M. Hansen, R. Tonkoski, M. Shirazi, R. Wies, and P. Cicilio, "Review of methods to accelerate electromagnetic transient simulation of power systems," *IEEE Access*, vol. 9, pp. 89714–89731, 2021.

[25] J. Lin and J. R. Marti, "Implementation of the CDA procedure in the EMTP," *IEEE Trans. Power Syst.*, vol. 5, no. 2, pp. 394–402, May 1990.

[26] Y. Xiaohui, T. Yong, and S. Qiang, "Variable order/step integration by 3-stage diagonally implicit Runge–Kutta method for electromagnetic transient simulations," *Power Syst. Technol.*, vol. 44, no. 11, pp. 4047–4054, 2020.

[27] J. Feng, W. Xiaoguang, and W. Xueguang, "State space method to analyze the electromagnetic transient of linear switching circuit," *Proc. CSEE*, vol. 36, no. 22, pp. 6028–6037, 2016.

[28] W. D. Humpage, K. P. Wong, T. T. Nguyen, and D. Sutanto, "Z-transform electromagnetic transient analysis in power systems," *IEE Proc. C, Gener., Transmiss. Distrib.*, vol. 127, no. 6, p. 370, 1980.

[29] J. Mahseredjian, V. Dinavahi, and J. A. Martinez, "Simulation tools for electromagnetic transients in power systems: Overview and challenges," *IEEE Trans. Power Del.*, vol. 24, no. 3, pp. 1657–1669, Jul. 2009.
[30] P. J. R. Balestero, J. S. L. Colqui, and S. Kurokawa, "Using the exact equivalent Π-circuit of transmission lines for electromagnetic transient simulations in the time domain," *IEEE Access*, vol. 10, pp. 90847–90856, 2022.

JING YE received the bachelor's degree from China Three Gorges University, in 2007, the master's degree from the School of Electrical and New Energy, China Three Gorges University, in 2010, and the Ph.D. degree from Wuhan University, in 2018. She was with the School of Electrical and New Energy, China Three Gorges University, from July 2010 to June 2013, where she is currently a Graduate Supervisor. She has published SCI/EI five search articles, 14 Chinese core articles, and two authorized Chinese invention patents. Her research interest includes the operation and control of power systems after large-scale new energy integration.

JIHAO XIE received the bachelor's degree from China Three Gorges University, in 2022, where he is currently pursuing the master's degree. His research interest includes electromagnetic transient simulation technology for new power systems.

YONG WANG received the bachelor's degree from the College of Science and Technology, China Three Gorges University, in 2015, and the master's degree from China Three Gorges University, in 2018. He is currently a member of the One-Level Team, State Grid Shanghai Electric Power Company, UHV Branch, where he engaged in research on modeling and simulation of HVDC transmission. He has published four SCI/EI search articles, 12 Chinese core articles, and one Chinese invention patent has been authorized.

LIANG ZHANG received the bachelor's degree from Gansu University of Technology, in 2004. He is currently the Chief Engineer with State Grid Qinghai Electric Power Company Ultra High Voltage Company. He is engaged in the operation and maintenance of ultra-high voltage converter stations and research on dc control and protection technology. He has published one SCI/EI search article, one Chinese core article, and has been granted one Chinese invention patent.

BINSHAN LI received the bachelor's degree from Wuhan University, in 2008. He is currently the Station Manager of the Ultra-High Voltage Qingnan Converter Station, State Grid Qinghai Electric Power Company. He is engaged in the operation and maintenance of the ultra-high voltage converter station and research on dc control and protection. He has published one SCI/EI search article, one Chinese core article, and two Chinese invention patents have been authorized.

JINWEI LV received the bachelor's degree from North China University of Water Resources and Hydropower, in 2006. Currently, he is the Deputy Team Leader of the Maintenance Center, State Grid Shanghai Electric Power Company, UHV Branch. He is engaged in research on the operation and inspection of UHV DC transmission converter station equipment. He has published three SCI/EI search articles, one Chinese core article, and two Chinese utility model patents that have been authorized.

KE LI received the bachelor's degree from Shaanxi University of Technology, in 2011. He is currently the Technical Specialist in the dc operation and maintenance with the Ultra-High Voltage Qingnan Converter Station, State Grid Qinghai Electric Power Company. He is engaged in the operation and maintenance of the ultra-high voltage converter station and related research. He has published some search articles and three Chinese invention patents have been authorized.

SHENGPENG JIN received the bachelor's degree from Tianjin University of Technology, in 2011. He is currently the Technical Specialist in the dc operation and maintenance with the Ultra-High Voltage Qingnan Converter Station, State Grid Qinghai Electric Power Company. He is engaged in the operation and maintenance of the ultra-high voltage converter station and related research. He has published one SCI/EI search article and six Chinese invention patents have been authorized.

YANG XU received the bachelor's degree from Taiyuan University of Science and Technology, in 2005, and the master's degree from Beijing Jiaotong University, in 2008. He is currently a member of the First Level Team, UHV Branch, State Grid Shanghai Electric Power Company, where he engaged in UHVDC transmission operation and maintenance work. He has published four core Chinese articles and has been granted one Chinese utility model patent.

WEI MA received the bachelor's degree from North China Electric Power University, in 2006. Currently, he is with the Operation and Inspection Department, Ultra High Voltage Converter Station Branch, Shanghai Electric Power Company. He has published more than three articles and several Chinese invention patents are under examination.